

Analytic studies of the complex Langevin equation with a Gaussian ansatz and multiple solutions in the unstable region

Yuya Abe and Kenji Fukushima

Department of Physics, The University of Tokyo, 7-3-1 Hongo, Bunkyo-ku, Tokyo 113-0033, Japan
(Received 25 July 2016; published 29 November 2016)

We investigate a simple model using the numerical simulation in the complex Langevin equation (CLE) and the analytical approximation with the Gaussian ansatz. We find that the Gaussian ansatz captures the essential and even quantitative features of the CLE results quite well when they converge to the exact answer, as well as the border of the unstable region where the CLE converges to a wrong answer. The Gaussian ansatz is therefore useful for looking into this convergence problem and we find that the exact answer in the unstable region is nicely reproduced by another solution that is naively excluded from the stability condition. We consider the Gaussian probability distributions corresponding to multiple solutions along the Lefschetz thimble to discuss the stability and the locality. Our results suggest a prescription to improve the convergence of the CLE simulation to the exact answer.

DOI: [10.1103/PhysRevD.94.094506](https://doi.org/10.1103/PhysRevD.94.094506)

I. INTRODUCTION

Functional integration in quantum field theories shares the same theoretical structure with the partition function in statistical mechanics and the Monte-Carlo algorithm is the most useful for both cases as long as the integrand is positive semidefinite. However, such an algorithm based on importance sampling in general breaks down for the integrand having an oscillating complex phase. This is the notorious sign problem and it unfortunately appears in many interesting physical environments such as quantum chromodynamics (QCD) at finite baryon chemical potential, QCD with a θ -term, Hubbard model away from the half filling, imbalanced or frustrated spin systems, etc. As found in reviews on the sign problem [1–6], many ideas have been proposed and tested, but no solution is established yet. For finite-density QCD, introductory lectures are available; see Ref. [7].

It would be a natural idea to seek for an alternative quantization scheme that is suitable for numerical simulations and does not rely on importance sample. One of the most promising candidates is the so-called stochastic quantization using the Langevin equation or the Fokker-Planck equation. A comprehensive review is found in Ref. [8]. An extension of the stochastic quantization procedure to a theory with complex terms is specifically referred to as the method of the complex Langevin equation (CLE), for the Langevin variables are complexified then (for the early pioneering attempt, see Ref. [9]). The potential of the CLE has been recently revisited as a theoretical tool to evade the sign problem in finite-density QCD (see Ref. [10] for a modern review). It was also expected that the CLE approach would be capable of describing real-time dynamics [11], but it was reported that the long-time numerical simulation falls into a wrong solution [11,12] (see also Ref. [13] for another real-time

subtlety to define the retarded and the advanced propagators with the CLE.) To identify the subtleties in the convergence problem in the CLE method, toy models have been quite useful to provide us with insights about the validity, which include low-dimensional models [14,15], (chiral) matrix models [15,16], and also even simple one-dimensional (or called zero-dimensional in the field-theory context) integrals [15,17–21], some of which are motivated by the sign problem for the Bose gas at finite chemical potential [22,23].

The breakthrough that triggered successful QCD (or gauge theory more generally) simulations such as pioneering, Refs. [24,25], and more recent, Refs. [26,27], was the recognition of the technique called the gauge cooling, which was introduced to make the probability distribution not spread in the complexified direction [28] [see also Ref. [29] for successful U(1) and SU(3) link model studies before the invention of the gauge cooling machinery], which may also cure the problem caused by the drift term singularity [15]. On the formal level the (sufficient) convergence criteria to the correct physical answer are known [19,30], which requires analyticity (holomorphicity) of the theory and the locality of the probability distribution.

It is sometimes quite instructive to consider the CLE method from the point of view of a similar complexified approach known as the Lefschetz thimble method as discussed in Refs. [21,31–34]. The Lefschetz thimble is a higher-dimensional extension of the steepest descent path in complex analysis and the most important property is that the complex phase is constant along this path or thimble (see Refs. [35] for mathematical foundation and also Refs. [36,37] for recent reviews). The method has been implemented for quantum field theory [38,39] and tested in low-dimensional models [40,41] (see also Ref. [42] for a condensed matter application). The important insight

obtained from the Lefschetz thimble method is that the Stokes phenomenon makes the structure of the theory complicated [43], which is the case near the phase transition or in the real-time formalism [33]. Another interesting observation is that there may appear multiple saddle points that have complex phases and their destructive interference [21,44] is indispensable to understand some nontrivial phenomenon like the Silver Blaze puzzle [45,46]. The strong advantage in the Lefschetz thimble method is that the analytical investigations are possible, which also leads to a new discovery of hidden theoretical structures [47].

The objective of this work is to explore some analytical aspects in the CLE approach. As compared to the Lefschetz thimble especially for the one-dimensional integral models, the CLE studies more often rely on numerical simulations. As closely discussed in Ref. [19] the probability distribution function can be constructed perturbatively, but to reveal the full profile, the numerical calculations are unavoidable, which is of course useful to deepen our understanding, but it would be desirable if we have analytical formulas from which we can somehow infer detailed information on the theory. To this end, we would propose a Gaussian ansatz in the present paper. This is a generalization of the mean-field treatment to the CLE framework. The idea can be traced back to a variational approach to stochastic quantization [48], and it was reported that an analytical evaluation with one variational parameter (corresponding to the dynamical mass) agrees quite well with the full numerical result for a one-dimensional N -component model. Within this variational approach the $1/N$ expansion has been also discussed in Ref. [49]. Such a mean-field treatment has been generalized to the CLE with a complex action for the relativistic Bose gas at finite chemical potential [23]. This direction of extension should be quite intriguing; for example, a comparison between the mean-field results and the CLE results in the Polyakov loop model has provided us with a useful hint on the breakdown of the CLE with a branch-cut crossing problem [50], and the more direct mean-field treatment of the CLE method itself would give us a further analytical insight into the subtlety of the convergence, as we will discuss. (For the Lefschetz thimble version of the comparison to the mean-field Polyakov loop model, see Ref. [51] which has justified the mean-field treatment in Ref. [52].)

This paper is organized as follows. In Sec. II basic equations of the CLE method are summarized for convenience of the readers and the Gaussian ansatz is introduced with two variational parameters as a generalization of the free two-point function. Section III is devoted to detailed explanations of the properties of the one-dimensional quartic model, followed by the main part of this paper in Sec. IV in which a comparison between the Gaussian ansatz results and the exact answer is made for three distinct regions of the model parameters. The conclusion is finally given in Sec. V.

II. FORMALISM

We briefly look over the general formalism of the complex Langevin method and its equivalent representation using the Fokker-Planck equation. Then, we introduce our idea of the Gaussian ansatz as an approximate solution of the Fokker-Planck equation. Here we will present expressions for a scalar field theory only, but the generalization for other field theories should be straightforward.

The fundamental ingredient in the complex Langevin method is a complexified extension of the Langevin equation with a fictitious time τ , which reads

$$\frac{\partial \phi(x, \tau)}{\partial \tau} = -\frac{\delta S[\phi]}{\delta \phi(x, \tau)} + \eta(x, \tau), \quad (1)$$

where $\eta(x, \tau)$ represents stochastic noise satisfying $\langle \eta(x, \tau) \eta(x', \tau') \rangle = 2\delta^{(d)}(x - x')\delta(\tau - \tau')$. If the action S takes a complex value, as is the case for fermions with a finite chemical potential or general real-time dynamics, ϕ should be also complexified as $\phi = \phi_R + i\phi_I$ with $\phi_R, \phi_I \in \mathbb{R}$. For analytical purposes it is often more convenient to deal with a different but equivalent representation of the quantization procedure using the Fokker-Planck equation, that is expressed as

$$\frac{dP[\phi]}{d\tau} = \int d^d x \left\{ \frac{\delta}{\delta \phi_R} \left[\text{Re} \left(\frac{\delta S}{\delta \phi} \right) P[\phi] \right] + \frac{\delta^2 P}{\delta \phi_R^2} + \frac{\delta}{\delta \phi_I} \left[\text{Im} \left(\frac{\delta S}{\delta \phi} \right) P[\phi] \right] \right\}. \quad (2)$$

For sign-problem free field theories in Euclidean space-time, the action S is a real functional of real ϕ and the solution of Eq. (2) approaches $P[\phi] \propto e^{-S[\phi]}$. In Minkowskian space-time, on the other hand, the action is complex (and another simple but useful example of a complex action is the Bose gas at finite chemical potential [22,23]). In a free real-time scalar theory, for an explicit example, S in momentum space is complex as

$$S[\phi] = i \int \frac{d^d p}{(2\pi)^d} \phi(-p)(-p^2 + m^2 - i\epsilon)\phi(p), \quad (3)$$

where a small real part is necessary for convergence in the $i\epsilon$ prescription. Obviously a real valued $P[\phi]$ cannot approach a standard form of the functional integral weight $\sim e^{-S[\phi]}$ because the weight is complex then. It is quite instructive that an analytical solution of the Fokker-Planck equation (2) is known for this example of Eq. (3) as [8]

$$P[\phi] = N \exp \left\{ - \int \frac{d^d p}{(2\pi)^d} \epsilon \left[\phi_R(-p)\phi_R(p) + \left(1 + \frac{2\epsilon^2}{(p^2 - m^2)^2} \right) \phi_I(-p)\phi_I(p) - \frac{2\epsilon}{p^2 - m^2} \phi_R(-p)\phi_I(p) \right] \right\}. \quad (4)$$

It is just a straightforward calculation to confirm that we can recover a correct expression for the propagator from this real probability weight, i.e.

$$\int \mathcal{D}\phi_R \mathcal{D}\phi_I P[\phi] \phi(-p) \phi(p) = \frac{i}{p^2 - m^2 + ie}. \quad (5)$$

We should note that the imaginary part in the right-hand side of Eq. (5) arises from not the weight $P[\phi]$ but complexified $\phi(p)$ in the left-hand side. Therefore, in such complexified representation of theory, the sign problem is evaded but the operator generally acquires a residual complex phase.

The prescription we would propose in this work is a Gaussian ansatz as an extension of Eq. (4), namely,

$$\epsilon \rightarrow A(p), \quad p^2 - m^2 \rightarrow -B(p) \quad (6)$$

for interacting field theories. Here, real-valued A and B are to be regarded as “renormalized” width and mass including interaction effects and should be determined by the stationary condition of the Fokker-Planck equation, that is; $dP/d\tau = 0$. Conceptually, the above ansatz should correspond to a Gaussian truncation with “mean-field” variables A and B optimized by the variational principle. Although this ansatz introduces an approximation, a fully analytical treatment is feasible then and it should be useful to understand how the complex Langevin equation converges to a false solution (which has been understood from power-decay behavior of the probability distribution [19] but we will shed light from a different perspective) and where we can find a correct answer (for successful applications of the mean-field treatment, see Ref. [23]).

III. QUARTIC MODEL

Here, a simplest one-dimensional (or in the field-theory context, it is commonly called “zero-dimensional” counting the number of spacetime) example should suffice for our present purpose to demonstrate how useful the Gaussian ansatz is to get an analytical insight.

A. Definition

We define the “theory” by the following integral [53];

$$\begin{aligned} Z(\alpha, \beta) &= \int d\phi e^{-S(\phi; \alpha, \beta)}, \\ S(\phi; \alpha, \beta) &= \frac{1}{2} \alpha \phi^2 + \frac{1}{4} \beta \phi^4, \end{aligned} \quad (7)$$

where $\alpha = a + ib$ ($a, b \in \mathbb{R}$) and $\beta = c + id$ ($c, d \in \mathbb{R}$) are complex coefficients and ϕ is a real integration variable. After the ϕ integration we can find the exact result in terms of the modified Bessel function as

$$Z(\alpha, \beta) = \sqrt{\frac{\alpha}{2\beta}} e^{\alpha^2/(8\beta)} K_{1/4}\left(\frac{\alpha^2}{8\beta}\right) \quad (8)$$

for $\text{Re}\alpha > 0$ and $\text{Re}\beta > 0$. For $\text{Re}\alpha < 0$ the Bessel function in the above expression should be replaced with $I_{\pm 1/4}(\frac{\alpha^2}{8\beta})$. For the validity check of the method, we will refer to the *exact answer* that we can obtain from these analytical expressions or from the direct numerical integration of Eq. (7).

This theory has interesting features similar to phase structures. To see them let us consider a two-point function, that is,

$$\begin{aligned} \langle \phi^2 \rangle_{\text{exact}} &= \frac{\int d\phi \phi^2 e^{-S}}{\int d\phi e^{-S}} \\ &= \frac{\alpha K_{-3/4}(\frac{\alpha^2}{8\beta}) + K_{5/4}(\frac{\alpha^2}{8\beta})}{4\beta K_{1/4}(\frac{\alpha^2}{8\beta})} - \frac{\alpha}{2\beta} - \frac{1}{\alpha} \end{aligned} \quad (9)$$

for $\text{Re}\alpha > 0$ and $\text{Re}\beta > 0$. Again, it is not difficult to carry out the direct numerical integration as long as $\text{Re}\beta > 0$. Now we see $\langle \phi^2 \rangle_{\text{exact}}$ as a function of $a = \text{Re}\alpha$ and $b = \text{Im}\alpha$ while keeping $\beta = 1$. Such a choice does not lose the generality because we can always rescale ϕ (after complexifying the theory) so that $\beta = 1$.

Figure 1 shows $|\langle \phi^2 \rangle_{\text{exact}}|$ as a function of a and b . It is clear to see that the expectation value increases in the region for $a < 0$, which is reminiscent of the spontaneous symmetry breaking. Of course, the present model does not have infinite degrees of freedom and, strictly speaking, the spontaneous symmetry breaking is impossible, i.e. $\langle \phi \rangle_{\text{exact}} = 0$ always holds for any a . Nevertheless, we can understand that a situation similar to the spontaneous symmetry breaking occurs in the following sense. The integration (7) is dominated around the minima (saddle

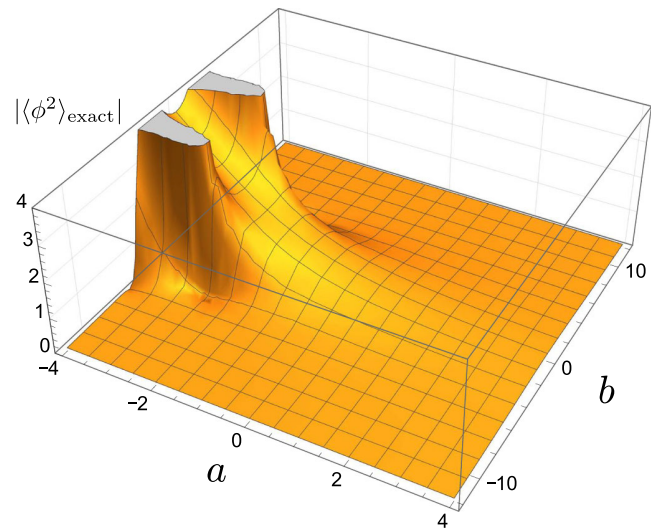


FIG. 1. Absolute value of the exact answer of $\langle \phi^2 \rangle_{\text{exact}}$ as a function of the real part a and the imaginary part b of the quadratic coefficient α .

points) of S as obtained from $dS/d\phi = 0$. For the present theory there are three saddle points,

$$\bar{\phi}_0 = 0, \quad \bar{\phi}_{\pm} = \pm\sqrt{-\alpha/\beta}. \quad (10)$$

Clearly $S = S_0 = 0$ at $\phi = \bar{\phi}_0$ and $S = S_{\pm} = -\alpha^2/4$ at $\phi = \bar{\phi}_{\pm}$. Therefore, as long as $\text{Re}S_{\pm} < \text{Re}S_0$, the integration is dominated around $\bar{\phi}_{\pm}$ and $\langle\phi^2\rangle_{\text{exact}}$ should behave like $-\alpha/\beta$ in the first approximation. There is no phase transition in a strict sense, but we may well identify this situation physically as an analogue of the *ordered state*.

The qualitative behavior, however, changes drastically at $|b| \simeq |a|$ with $a < 0$ and, so to speak, the broken symmetry is restored in the region for $|b| > |a|$. The reason for this change is easy to understand from the above consideration. For $|b| > |a|$ we explicitly see $\text{Re}S_{\pm} = -a^2 + b^2 > \text{Re}S_0 = 0$, and so the integration is again dominated around $\bar{\phi}_0$ and the nonzero expectation values at $\bar{\phi}_{\pm}$ become irrelevant in effect. Thus, we may say that the ordered state is hindered by attenuation effects caused by large b .

In summary this theory has three characteristic and qualitatively distinct states depending on a and b as follows:

$$\begin{aligned} a > 0: & \text{ normal state} \\ a < 0, \quad a^2 \gtrsim b^2: & \text{ ordered state} \\ a < 0, \quad b^2 \gtrsim a^2: & \text{ attenuated state.} \end{aligned}$$

It is known that the CLE fails in the attenuated state for $a < 0$ and $b^2 \gtrsim a^2$, which we will closely investigate analytically using the Gaussian ansatz. Also, it would be worthwhile mentioning that the convergence of the CLE simulation to the exact answer is proven in the region with $a > 0$ and $b^2 < 3a^2$, while the CLE simulation may not work for higher order expectation values, $\langle\phi^n\rangle$ ($n \geq 4$), in the region with $a > 0$ and $b^2 > 3a^2$ even in the normal state [19]. For the moment we will focus on $\langle\phi^2\rangle$ and will test our method for $\langle\phi^4\rangle$ later.

B. Results from the CLE

Here, we briefly discuss the results from the CLE to show where the CLE fails (for the two-point function). We numerically solved Eq. (1) for the action (7) with discretization $dt = 5 \times 10^{-3}$ and updated the fictitious time evolution by 10^5 steps and average the numerical outputs over time. When we detected a runaway trajectory, we decreased the step size and took 10^3 steps back to avoid contamination from the runaway.

We show the difference between the CLE results and the exact answer in Fig. 2. From this comparison we see that the CLE works good for $a > 0$ generally (there may be a failure for the higher order functions [19] and we will come

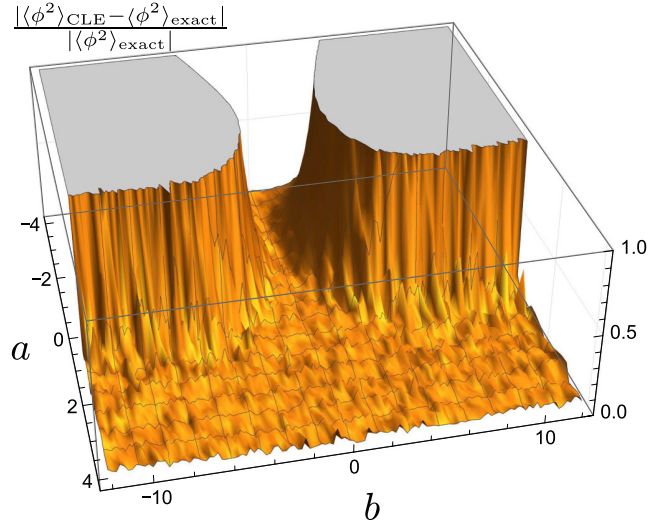


FIG. 2. Comparison between the CLE results and the exact answer.

to this point in the end of this paper), and also it works in the ordered state with $a < 0$ as long as $a^2 > b^2$. We just note that in this theory the Stokes phenomenon occurs at $a = 0$, and so the onset of the Stokes phenomenon does not necessarily coincide with the breakdown of the CLE simulation. As we mentioned before, the most problematic region for the CLE calculation in this theory is $a < 0$ and $b^2 \gtrsim a^2$, which we call the attenuated state throughout this present work.

IV. ANALYSIS WITH THE GAUSSIAN ANSATZ

Because the Gaussian ansatz is not an exact solution of the Fokker-Planck equation (2) for $\beta \neq 0$ in general, there is some ambiguity in the determination of A and B associated with the choice of what we optimize. A prescription we adopt here is an equilibrium condition for a two-point function, that is,

$$\int d\phi_R d\phi_I \phi^2 \frac{dP[\phi]}{d\tau} = 0, \quad (11)$$

which naturally must hold when $dP[\phi]/d\tau = 0$ is reached. From the real and the imaginary parts of the above condition, we can get two equations to solve A and B as functions of a and b . It should be noted that this condition has similarity to the ‘‘criteria for correctness’’ of the second order as discussed in Ref. [19]. Thus our condition naturally leads to a sort of gap equation in a sense that the n th order criteria for correctness is equivalent to the Schwinger-Dyson equation of n -point function.

A. Normal state

Plugging the action (7) into the Fokker-Planck equation (2), we can express $dP/d\tau$ and substitute it for

Eq. (11). We can explicitly perform the Gaussian integrations with respect to ϕ_R and ϕ_I and after simplifying terms, we can find a set of equations to fix $A(\alpha, \beta)$ and $B(\alpha, \beta)$ as

$$A - a = \frac{3}{A^2 + B^2}(cA + dB), \quad (12)$$

$$B - b = \frac{3}{A^2 + B^2}(dA - cB). \quad (13)$$

It is easy to confirm that the noninteracting limit at $\beta = 0$ (i.e. $c = d = 0$) immediately leads to $A(\alpha, 0) = a$ and $B(\alpha, 0) = b$ as it should (and this free solution is nothing but the lowest order solution discussed in Ref. [19]).

There are four independent branches of solutions for Eq. (13). For our present choice of $\beta = 1$ (i.e. $c = 1$ and $d = 0$) the above set of equations leads to two complex and two real solutions. The real solution with $A > 0$, which is required for the stability of the Gaussian integration, is uniquely determined as

$$A = \frac{a}{2} + \frac{1}{2\sqrt{2}} \sqrt{\sqrt{48a^2 + (a^2 + b^2 - 12)^2} + a^2 - b^2 + 12}, \quad (14)$$

$$B = \frac{b}{2} + \frac{\text{sgn}(ab)}{2\sqrt{2}} \times \sqrt{\sqrt{48a^2 + (a^2 + b^2 - 12)^2} - a^2 + b^2 - 12}. \quad (15)$$

It is clear that we can give an estimate for the two-point function using the Gaussian ansatz in the following way:

$$\begin{aligned} \langle \phi^2 \rangle_{\text{Gauss}} &= \frac{\int d\phi_R d\phi_I \phi^2 P[\phi]}{\int d\phi_R d\phi_I P[\phi]} \\ &= \frac{1}{A(\alpha, \beta) + iB(\alpha, \beta)}. \end{aligned} \quad (16)$$

This final result from the Gaussian ansatz is so simple in the analytical structure as compared to the exact answer, but we can confirm that this gives a good approximation in the normal state.

To quantify how good the Gaussian ansatz is, let us make a plot in a way similar to Fig. 2, with $\langle \phi^2 \rangle_{\text{CLE}}$ replaced with $\langle \phi^2 \rangle_{\text{Gauss}}$, which is presented in Fig. 3. It is very interesting to see that Fig. 3 has a remarkable similarity to Fig. 2. In particular the Gaussian ansatz works excellently to show good agreement with the exact answer in the region with $a \geq 0$ for any b . The next question that naturally arises is how close to each other $\langle \phi^2 \rangle_{\text{Gauss}}$ and $\langle \phi^2 \rangle_{\text{CLE}}$ are in the whole region, especially whether “wrong” values in the attenuated state agree or not. We numerically checked this

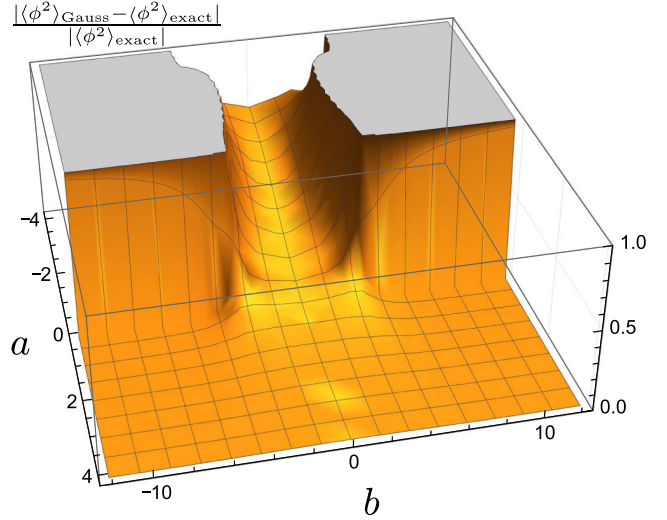


FIG. 3. Comparison between the Gaussian ansatz results and the exact answer for the quadratic operator.

to find that they are different approximately by a factor 3. Later, we will discuss how to reach the exact answer in the attenuated state.

Our Gaussian ansatz takes care of fluctuations around $\bar{\phi}_0$ and implicitly neglects the contributions from other saddle points at $\bar{\phi}_\pm$. In terms of the Lefschetz thimble method, such an approximated treatment is justified by the fact that only the thimble attached to $\bar{\phi}_0$ makes a finite contribution for $a > 0$. There is, however, a sudden change in the thimble structure at $a = 0$, which is commonly called the Stokes phenomenon, and eventually all three thimbles attached to $\bar{\phi}_0$ and $\bar{\phi}_\pm$ come to make a finite contribution for $a < 0$. This sudden change partially explains the sudden breakdown of the Gaussian ansatz estimate around $a = 0$.

One might have an impression that the Gaussian ansatz may still work in the ordered state in view of Fig. 3 but some cautions are needed. In the region with $a^2 > b^2$ and $a < 0$, as $|a|$ grows up (and so the “condensate” grows up), the agreement gets worse. For example, at $a = -4$ and $b = 0$ as shown in Fig. 3, $|\langle \phi^2 \rangle_{\text{Gauss}} - \langle \phi^2 \rangle_{\text{exact}}| / |\langle \phi^2 \rangle_{\text{exact}}| \approx 0.5$ and the deviations would be larger with increasing $|a|$ in the negative direction. However, as we see from Fig. 2, the CLE should describe the physics correctly also in this region of the ordered state.

B. Ordered state

In many physical examples the Stokes phenomenon makes the difficulty even more difficult. However, the CLE is capable of going beyond the Stokes phenomenon from the normal state to the ordered state except for the onset region. Although the most interesting question is what should be happening in the attenuated state as we will address later, let us clarify how the Gaussian ansatz can capture the correct physics in the ordered state too.

In this region the contributions around $\bar{\phi}_{\pm}$ should be dominant, and so the Gaussian ansatz must be formulated also around $\bar{\phi}_{\pm}$. In the mean-field-type calculations it is a common technique to consider fluctuations around a shifted vacuum that is self-consistently determined by the energy minimization condition. Therefore, the probability weight should be changed as $P[\phi] \rightarrow P_{\pm}[\phi] = P[\phi + \bar{\phi}_{\pm}]$ with A_{\pm} and B_{\pm} . Then, the two-point function should be approximated as

$$\langle \phi^2 \rangle_{\text{Gauss}} = \frac{1}{A_{\pm} + iB_{\pm}} - \frac{\alpha}{\beta}, \quad (17)$$

where the last term represents the contribution by $\bar{\phi}_{\pm}^2 = -\alpha/\beta$. The set of equations to fix A_{\pm} and B_{\pm} is slightly changed from Eq. (13) by $\bar{\phi}_{\pm}^2$ as

$$A_{\pm} + 2a = \frac{3}{A_{\pm}^2 + B_{\pm}^2} (cA_{\pm} + dB_{\pm}), \quad (18)$$

$$B_{\pm} + 2b = \frac{3}{A_{\pm}^2 + B_{\pm}^2} (dA_{\pm} - cB_{\pm}). \quad (19)$$

We can solve the above easily to find the analytical expressions again.

Here, let us make a remark on the convergence to the right solution. Generally speaking, beyond the Stokes phenomenon, multiple saddle points take part in the integration; all of $\bar{\phi}_0$ and $\bar{\phi}_{\pm}$ in the present case. In physical applications it is often the case that one of them dominates the physics. The spontaneous symmetry breaking is such a phenomenon that can be correctly described by one saddle-point property. Because our one-dimensional theory does not have such symmetry breaking, we have to sum up both contributions from $\bar{\phi}_{\pm}$ to have $\langle \phi \rangle = 0$, but with infinite degrees of freedom only one contribution is spontaneously chosen, and thus the CLE method should work better than. Some other special examples are known to be more problematic. The mixed phase associated with a first-order phase transition should be one of the most typical examples. In such a situation contributions from different saddle points are equally important, and also missing a relative complex phase may cause a further problem of falling into a wrong answer [21]. Another famous example is the Silver Blaze problem for which relative phases from infinite saddle points make destructive interference [44]. For these problems, to formulate the Gaussian ansatz to work, we need to take a proper superposition of $P_0[\phi]$ centered at $\bar{\phi}_0$ and $P_{\pm}[\phi]$ centered at $\bar{\phi}_{\pm}$ with relative weights including complex phase factors.

C. Attenuated state

The most interesting and nontrivial question is why the CLE simulation and also the Gaussian ansatz do not work

in the attenuated state with $a < 0$ and $b^2 \gtrsim a^2$. This is beyond the Stokes phenomenon, but because of the real weight, $e^{-\text{Re}S} = e^{-(b^2 - a^2)/4} \ll 1$, we can safely neglect these contributions from $\bar{\phi}_{\pm}$ for $b^2 \gg a^2$ and the integration should be well approximated by the fluctuations around $\bar{\phi}_0$ only. Thus, it is very likely that the CLE simulation and the Gaussian ansatz should be valid descriptions, but they fail in practice. Because the Gaussian ansatz enables us to cope with the problem with simple analytical formulas, we can relatively easily identify the source of the problem.

It is already apparent from Eq. (15) how the Gaussian ansatz leads to unphysical behavior. Let us consider expected behavior of B for asymptotically large b . Naturally, we would immediately anticipate $B \simeq b$ for large enough b from our physical intuition, and Eq. (15) indeed predicts $B \rightarrow b$ for $|b| \gg a$ as long as $a > 0$, while it gives $B \rightarrow 0$ for $|b| \gg |a|$ once the system enters $a < 0$. This is a very clear manifestation of where the wrong answer is picked up. Actually, the exact answer certainly exhibits the behavior of $B \simeq b$ even in the $a < 0$ region, as checked in Fig. 4 where a counterpart of B defined by $\text{Im}(\langle \phi^2 \rangle_{\text{exact}})^{-1}$ is plotted as a function of a and b . Apart from the ordered state for $a < 0$, $a^2 > b^2$ and some spiky structures near the phase border, $\text{Im}(\langle \phi^2 \rangle_{\text{exact}})^{-1}$ clearly scales as $\sim b$ in a way consistent with our intuition.

We already pointed out that there is another real solution of the set of equations (13), whose explicit forms are

$$\tilde{A} = \frac{a}{2} - \frac{1}{2\sqrt{2}} \sqrt{\sqrt{48a^2 + (a^2 + b^2 - 12)^2} + a^2 - b^2 + 12}, \quad (20)$$

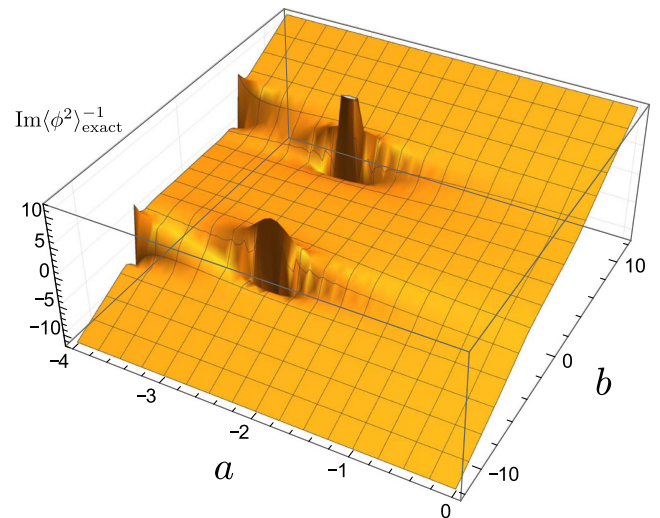


FIG. 4. Counterpart of B inferred from $\langle \phi^2 \rangle_{\text{exact}}$ as a function of a and b in the region for $a < 0$.

$$\tilde{B} = \frac{b}{2} - \frac{\text{sgn}(ab)}{2\sqrt{2}} \times \sqrt{\sqrt{48a^2 + (a^2 + b^2 - 12)^2} - a^2 + b^2 - 12}. \quad (21)$$

The problem of this solution is that the integration with the Gaussian probability is not well defined due to $\tilde{A} < 0$ and we should usually exclude this branch of the solution.

For the moment let us postpone discussions on the stability but simply adopt the above branch of solution to evaluate new $\langle \tilde{\phi}^2 \rangle_{\text{Gauss}} = 1/(\tilde{A} + i\tilde{B})$ in the $a < 0$ region. We show the comparison between $\langle \tilde{\phi}^2 \rangle_{\text{Gauss}}$ and the exact answer in Fig. 5 and it is clear from this comparison that this new $\langle \tilde{\phi}^2 \rangle_{\text{Gauss}}$ gives a very good approximation in the region with $a < 0$ and $b^2 > a^2$ (if sufficiently away from the phase boundary; see also the structure in Fig. 4). The important observation is that we take the difference between $\langle \tilde{\phi}^2 \rangle_{\text{Gauss}}$ and $\langle \phi^2 \rangle_{\text{exact}}$ before computing its absolute value, and so the good agreement seen in Fig. 5 includes the information on the complex phase. This means that, even though $\tilde{A} < 0$ seems to be not allowed for convergence of the Gaussian integral, the exact answer indicates that this seemingly unstable $\tilde{A} < 0$ is actually the right physical branch of solution.

Then, two questions arise. One is how such an unstable branch of solution can be the physical choice. Another one is what principle determines which branch of solution describes physically the correct behavior of the theory. These questions cannot be answered within the framework of the CLE or the Gaussian ansatz of the CLE but we need more inputs from different approaches. Here, let us

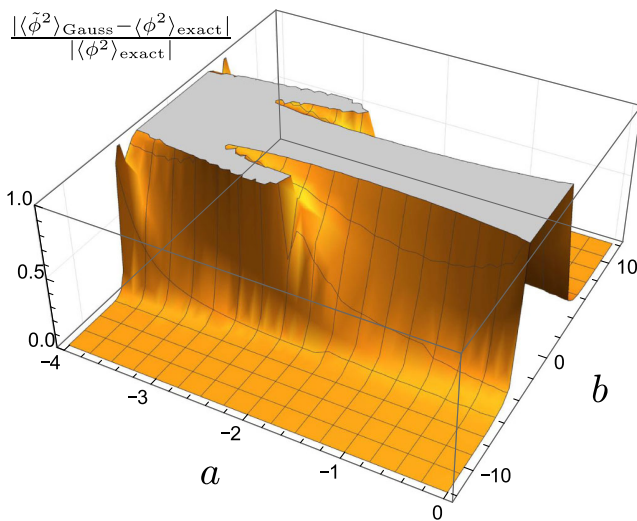


FIG. 5. Comparison in the $a < 0$ region between the Gaussian ansatz results with the unstable branch of solution and the exact answer.

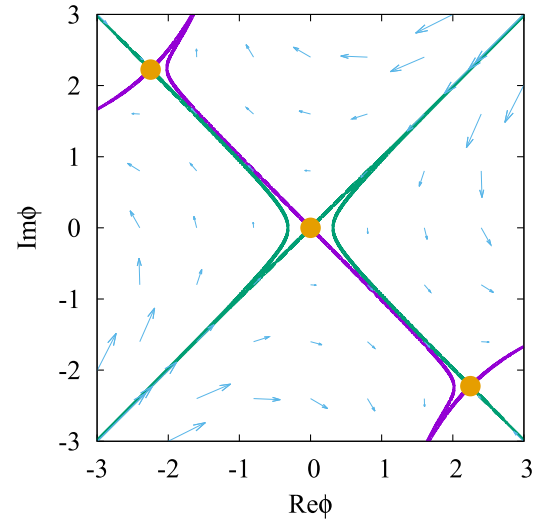


FIG. 6. Steepest descendent paths (Lefschetz thimbles) shown by purple lines and steepest ascendent paths shown by green lines around three saddle points shown by orange dots. Parameters are chosen as $a = -0.1$ and $b = 10$.

consider these questions by means of the Lefschetz thimble method. Figure 6 is a typical example of the thimble structures in the attenuated state for $a < 0$ and $b^2 \gg a^2$, and to draw Fig. 6 we chose $a = -0.1$ and $b = 10$. From this we understand that the integration path along the thimble or the steepest descendent path is tilted from the real axis by $-\pi/4$ around $\bar{\phi}_0 = 0$ if $a < 0$ and $b^2 \gg a^2$.

Because we already know that the integral is dominated by the contribution near $\bar{\phi}_0$ only, we shall change the integration variable along the “thimble-inspired” integration path (that coincides with the Lefschetz thimble near $\bar{\phi}_0$) as

$$\phi \rightarrow \phi' = e^{i\pi/4} \phi. \quad (22)$$

Let us point out that such a U(1) rotation makes sense only in the complexified description and this kind of transformation may be linked to the gauge cooling in the gauge theory. Then, the action (7) near $\bar{\phi}_0$ is expressed as

$$S \simeq \frac{1}{2}(-i\alpha)\phi'^2 = \frac{1}{2}(b - i\alpha)\phi'^2, \quad (23)$$

which implies that the roles of a and b should be switched to each other along this path. Needless to say, such a variable change causes another convergence problem from the ϕ^4 term in the definition of the theory, but we are focusing only on the local properties around $\bar{\phi}_0$. Such a treatment shall be self-consistently justified if the probability distribution is localized well around $\bar{\phi}_0$. Now, because of Eq. (23), the probability distribution in the Gaussian ansatz should be parametrized by B' instead of A and $-A'$ instead of B . Equation (13) should be also replaced as

$$B' - b = \frac{3}{A^2 + B^2} \cdot (-B'), \quad (24)$$

$$-A' + a = \frac{3}{A^2 + B^2} (-A'), \quad (25)$$

where $c = -1$ (after the change of $\phi \rightarrow \phi'$) and $d = 0$ are plugged in. Then, the above equations are completely identical to the original equations (13) having the same solutions of Eqs. (14) and (15), and Eqs. (20) and (21). Even though the solutions are just the same, this argument tells us an important implication—for the integration with the Gaussian ansatz to converge around $\bar{\phi}_0$, what we need is $B > 0$ and the sign of A does not matter. In this way, the first question is answered now. Both branches of A , B and \tilde{A} , \tilde{B} are possible; Eqs. (15) and (21) lead to $B > 0$ and $\tilde{B} > 0$ for $b > 0$. We note that the thimble would be tilted in the opposite direction for $b < 0$ and then the convergence would require $B < 0$ and $\tilde{B} < 0$ which are also satisfied in Eqs. (15) and (21).

The second question is a little more nontrivial; both solutions seem to be equally possible from the integration stability condition. Besides, in the $a > 0$ region, we have chosen Eqs. (14) and (15) from the condition of $A > 0$ in the previous discussion, but even in this $A > 0$ case, once we consider the path deformation along the Lefschetz thimble, the convergence condition around $\bar{\phi}_0$ is only the realness of A and B . Hence, regardless of the sign of A , both solutions, Eqs. (14) and (15) and Eqs. (20) and (21), are possible.

For the self-consistent justification, the Gaussian width must be small. The Gaussian width along the thimble near $\bar{\phi}_0$ is determined by $\sqrt{A^2 + B^2}$, and interestingly, we can readily find from Eqs. (14) and (15), and Eqs. (20) and (21), that

$$\begin{aligned} \sqrt{A^2 + B^2} &\gg \sqrt{\tilde{A}^2 + \tilde{B}^2} \quad \text{for } a > 0, \\ \sqrt{\tilde{A}^2 + \tilde{B}^2} &\gg \sqrt{A^2 + B^2} \quad \text{for } a < 0. \end{aligned} \quad (26)$$

This observation nicely explains which branch of solution should be picked up to describe the correct physics. For the demonstration purpose to visualize how the probability distributions spread, we plot $P[\phi']$ along the thimble in terms of ϕ' in Fig. 7 and from this plot we see that the spreading distribution with Eqs. (14) and (15) is not very well localized around $\bar{\phi}_0$ but it is stretched to the regions around $\bar{\phi}_\pm$, which already signals for falling into a wrong answer.

An interesting question is what then happens if we implement the CLE simulation after performing a rotation like Eq. (23) or more generally: $S[\phi'] = \frac{1}{2}|\alpha|\phi'^2 + \frac{1}{4}\beta e^{-2i\theta}\phi'^4$ where θ is an argument of a complex number α and $\phi' = e^{i\theta/2}\phi$. Such a deformation of the theory might

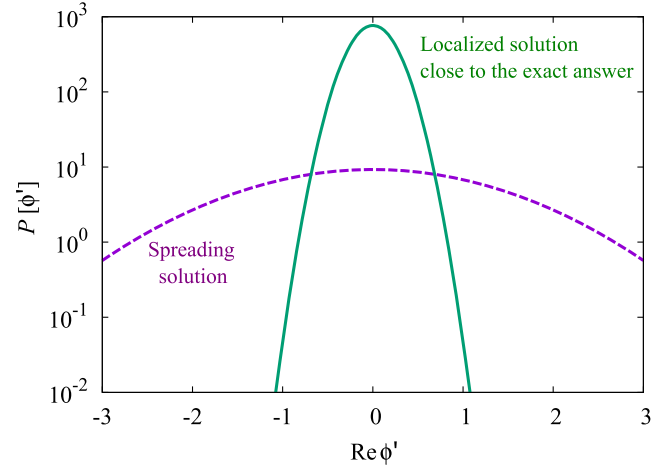


FIG. 7. Gaussian profiles along the thimble-inspired path near $\bar{\phi}_0$ corresponding to Eqs. (14) and (15) (spreading solution by the dotted line) and Eqs. (20) and (21) (localized solution by the solid line) for $a = -0.1$ and $b = 10$.

make the existence of the theory questionable, but we should remember that the existence of the theory is already subtle as soon as it is complexified because the complexified stochastic processes may always hit diverging rays on the complex plane; for the existence of the theory due to the cancellation of divergences, see discussions in Sec. 11.5 in Ref. [8]. We may also say that we could have put a small ϕ'^4 term in the probability distribution that guarantees the convergence, which is dropped in the Gaussian ansatz.

Figure 8 shows our CLE results along the tilted path in terms of ϕ' . The structure for $a < 0$ is surprisingly similar to the results in the Gaussian ansatz with \tilde{A} and \tilde{B} presented in Fig. 5. This is a very clear numerical evidence about such a close relation between the CLE and the Gaussian ansatz

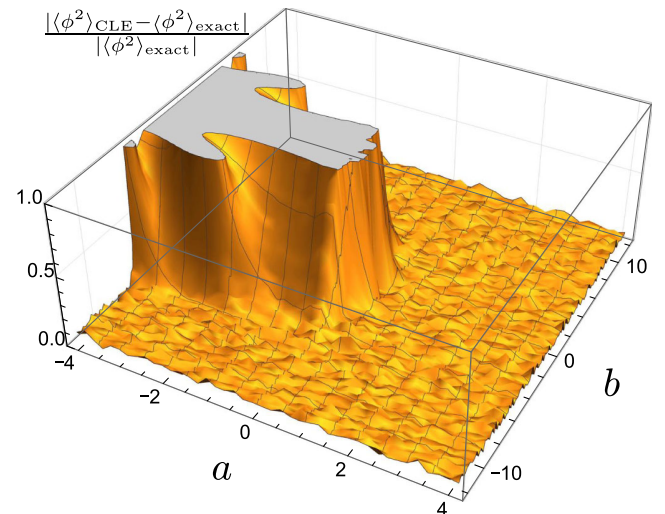


FIG. 8. Comparison between the CLE results along the Lefschetz thimble and the exact answer for the quadratic operator.

results. Summarizing our findings, the failure of the CLE simulation in the attenuated state as seen in Fig. 2 is attributed to the seemingly more stable but unphysically spreading solution, and if the CLE simulation is performed along the Lefschetz thimble without phase oscillation, the physical well-localized solution is correctly picked up to recover the exact answer. We note that we simplified the treatment by performing the thimble-inspired rotation only but it is in principle feasible to change the variable more faithfully to the Lefschetz thimble. Again, we would emphasize that our proposed simple treatment of the Gaussian ansatz is so powerful to explain all the good and bad behavior of the CLE simulations (where it works quantitatively for good behavior and only qualitatively for bad behavior).

Another interesting and important question is whether the Gaussian ansatz works for higher order operators or not. It has been argued in Ref. [19] that $\langle \phi^4 \rangle$ cannot converge to the physical answer for $b^2 > 3a^2$ even in the $a > 0$ region, while $\langle \phi^2 \rangle$ can. Our optimistic guess is that the Gaussian ansatz should be a valid description for higher order operators because the probability distribution is exponentially localized by construction. It is quite easy to check it by a generalization of Eq. (16), i.e.

$$\langle \phi^4 \rangle_{\text{Gauss}} = \frac{3}{[A(\alpha, \beta) + iB(\alpha, \beta)]^2}. \quad (27)$$

Then, the comparison to the exact answer is shown in Fig. 9, which looks just like the comparison for $\langle \phi^2 \rangle$ in Fig. 3. From this explicit comparison it is obvious that the Gaussian ansatz definitely remains as a good approximation even for higher order operators in the region with $a > 0$ and $b^2 > 3a^2$.

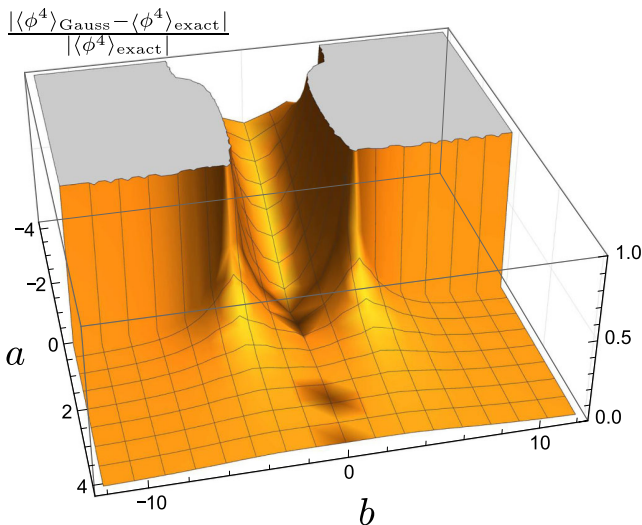


FIG. 9. Comparison between the Gaussian ansatz results and the exact answer for the quartic operator.

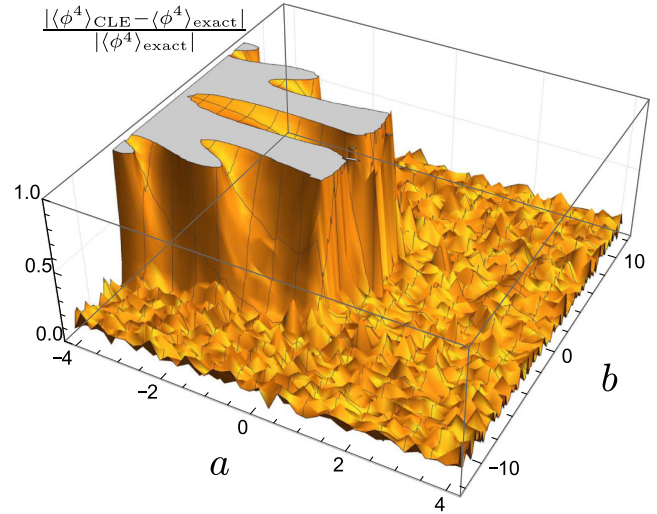


FIG. 10. Comparison between the CLE results along the Lefschetz thimble and the exact answer for the quartic operator.

Now, a natural question is what happens in the numerical CLE simulation for $\langle \phi^4 \rangle$. If the original action is put into the CLE simulation, we can indeed see sizable deviations of $\langle \phi^4 \rangle_{\text{CLE}}$ from the exact answer even at $a > 0$ in the $b^2 \gg a^2$ region. If the simulation goes to higher and higher order operators, the failure region expands toward $b^2 > 3a^2$ gradually. Now, the most interesting question is whether the transformation from ϕ to ϕ' can help the CLE simulation with approaching the exact answer. Figure 10 shows such a comparison. Surprisingly, it is evident that the convergence problem in the $a > 0$ region has been completely resolved.

V. CONCLUSION

We have exploited an approximation scheme using the Gaussian ansatz to solve the Fokker-Planck equation and made quantitative comparisons between the complex Langevin equation, CLE, results and the Gaussian ansatz results. Although the gap equations in the Gaussian ansatz are so simple, we have confirmed that multiple solutions from them capture all the essential features of the CLE simulation not only for the successful regions quantitatively but also for the unsuccessful regions qualitatively.

Our most striking finding is that one poorly localized branch of solutions is picked up by the Gaussian ansatz and another branch of solutions corresponds to the correct physical answer in the unsuccessful parameter regions. To pick the correct one up, if the theory is reexpressed in terms of the variable along the Lefschetz thimble (though it was done only approximately in the present work), the branch of solution that describes a more localized probability distribution can be picked up, which has been revealed by multiple solution structures in the Gaussian ansatz. The

idea has been tested in the CLE simulation also, and we have verified the consistency between the thimble-guided CLE simulation and the physical branch of solutions in the Gaussian ansatz.

Our analysis implies a positive prospect in favor of the CLE simulation. Even when the convergence property is not sufficiently good leading to unphysical results, it does not necessarily mean the complete breakdown of the method itself. When it occurs, the CLE simulation may have multiple fixed points and it simply falls into where it should not fall into, though one of other fixed points may still correspond to the correct physics. This is very nice, because a minimal change in the treatment like the deformation of the integration path could help us with digging out the correct branch of solutions (see also the results in Refs. [18,34] for other minimal changes to improve the correct convergence). This observation might

have something to do with recently proposed ideas on the gauge cooling for the singular-drift problem [15]. It would be the most exciting challenge to apply our method of the Gaussian ansatz to another theory like $S = -(\beta \cos \theta + i\theta)$ [54] which is the simplest integral that emulates the symmetry properties of lattice gauge theories.

ACKNOWLEDGMENTS

The authors thank Gert Aarts, Yoshimasa Hidaka, Jan Pawłowski, and Yuya Tanizaki for useful discussions and comments. K. F. is grateful for warm hospitality at Institut für Theoretische Physik, Universität Heidelberg, where K. F. stayed as a visiting professor of EMMI-ExtreMe Matter Institute/GSI and a part of this work was completed. This work was partially supported by JSPS KAKENHI Grants No. 15H03652 and No. 15K13479.

-
- [1] E. Y. Loh, J. E. Gubernatis, R. T. Scalettar, S. R. White, D. J. Scalapino, and R. L. Sugar, Sign problem in the numerical simulation of many-electron systems, *Phys. Rev. B* **41**, 9301 (1990).
- [2] S. Muroya, A. Nakamura, C. Nonaka, and T. Takaishi, Lattice QCD at finite density: An introductory review, *Prog. Theor. Phys.* **110**, 615 (2003).
- [3] S. Ejiri, Recent progress in lattice QCD at finite density, *Proc. Sci.*, LATTICE2008 (2008) 002 [arXiv:0812.1534].
- [4] K. Fukushima and T. Hatsuda, The phase diagram of dense QCD, *Rep. Prog. Phys.* **74**, 014001 (2011).
- [5] P. de Forcrand, Simulating QCD at finite density, *Proc. Sci.*, LAT2009 (2009) 010 [arXiv:1005.0539].
- [6] G. Aarts, Complex Langevin dynamics and other approaches at finite chemical potential, *Proc. Sci.*, LATTICE2012 (2012) 017 [arXiv:1302.3028].
- [7] G. Aarts, Introductory lectures on lattice QCD at nonzero baryon number, *J. Phys. Conf. Ser.* **706**, 022004 (2016).
- [8] P. H. Damgaard and H. Hufel, Stochastic quantization, *Phys. Rep.* **152**, 227 (1987).
- [9] F. Karsch and H. W. Wyld, Complex Langevin Simulation of the SU(3) Spin Model With Nonzero Chemical Potential, *Phys. Rev. Lett.* **55**, 2242 (1985).
- [10] G. Aarts, L. Bongiovanni, E. Seiler, D. Sexty, and I. O. Stamatescu, Controlling complex Langevin dynamics at finite density, *Eur. Phys. J. A* **49**, 89 (2013).
- [11] J. Berges and I.-O. Stamatescu, Simulating Nonequilibrium Quantum Fields with Stochastic Quantization Techniques, *Phys. Rev. Lett.* **95**, 202003 (2005); J. Berges, S. Borsanyi, D. Sexty, and I.-O. Stamatescu, Lattice simulations of real-time quantum fields, *Phys. Rev. D* **75**, 045007 (2007); J. Berges and D. Sexty, Real-time gauge theory simulations from stochastic quantization with optimized updating, *Nucl. Phys.* **B799**, 306 (2008).
- [12] R. Anzaki, K. Fukushima, Y. Hidaka, and T. Oka, Restricted phase-space approximation in real-time stochastic quantization, *Ann. Phys. (Amsterdam)* **353**, 107 (2015).
- [13] K. Fukushima and T. Hayata, Schwinger mechanism with stochastic quantization, *Phys. Lett. B* **735**, 371 (2014).
- [14] J. M. Pawłowski and C. Zielinski, Thirring model at finite density in $0+1$ dimensions with stochastic quantization: Crosscheck with an exact solution, *Phys. Rev. D* **87**, 094503 (2013); Thirring model at finite density in $2+1$ dimensions with stochastic quantization, *Phys. Rev. D* **87**, 094509 (2013).
- [15] K. Nagata, J. Nishimura, and S. Shimasaki, Justification of the complex Langevin method with the gauge cooling procedure, *Prog. Theor. Exp. Phys.* (2016) 013B01; K. Nagata, J. Nishimura, and S. Shimasaki, Gauge cooling for the singular-drift problem in the complex Langevin method—A test in random matrix theory for finite density QCD, *J. High Energy Phys.* **07** (2016) 073; The argument for justification of the complex Langevin method and the condition for correct convergence, arXiv:1606.07627.
- [16] A. Mollgaard and K. Splittorff, Complex Langevin dynamics for chiral random matrix theory, *Phys. Rev. D* **88**, 116007 (2013); Full simulation of chiral random matrix theory at nonzero chemical potential by complex Langevin, *Phys. Rev. D* **91**, 036007 (2015).
- [17] G. Aarts and K. Splittorff, Degenerate distributions in complex Langevin dynamics: One-dimensional QCD at finite chemical potential, *J. High Energy Phys.* **08** (2010) 017.
- [18] G. Aarts, F. A. James, J. M. Pawłowski, E. Seiler, D. Sexty, and I. O. Stamatescu, Stability of complex Langevin dynamics in effective models, *J. High Energy Phys.* **03** (2013) 073.
- [19] G. Aarts, P. Giudice, and E. Seiler, Localized distributions and criteria for correctness in complex Langevin dynamics, *Ann. Phys. (Amsterdam)* **337**, 238 (2013).

- [20] J. Nishimura and S. Shimasaki, New insights into the problem with a singular drift term in the complex Langevin method, *Phys. Rev. D* **92**, 011501 (2015).
- [21] T. Hayata, Y. Hidaka, and Y. Tanizaki, Complex saddle points and the sign problem in complex Langevin simulation, *Nucl. Phys.* **B911**, 94 (2016).
- [22] G. Aarts, Can Stochastic Quantization Evade the Sign Problem? The Relativistic Bose Gas at Finite Chemical Potential, *Phys. Rev. Lett.* **102**, 131601 (2009).
- [23] G. Aarts, Complex Langevin dynamics at finite chemical potential: Mean field analysis in the relativistic Bose gas, *J. High Energy Phys.* **05** (2009) 052.
- [24] D. Sexty, Simulating full QCD at nonzero density using the complex Langevin equation, *Phys. Lett. B* **729**, 108 (2014).
- [25] G. Aarts, E. Seiler, D. Sexty, and I. O. Stamatescu, Simulating QCD at nonzero baryon density to all orders in the hopping parameter expansion, *Phys. Rev. D* **90**, 114505 (2014).
- [26] Z. Fodor, S. D. Katz, D. Sexty, and C. Torok, Complex Langevin dynamics for dynamical QCD at nonzero chemical potential: A comparison with multiparameter reweighting, *Phys. Rev. D* **92**, 094516 (2015).
- [27] G. Aarts, F. Attanasio, B. Jaeger, and D. Sexty, The QCD phase diagram in the limit of heavy quarks using complex Langevin dynamics, *J. High Energy Phys.* **09** (2016) 087.
- [28] E. Seiler, D. Sexty, and I. O. Stamatescu, Gauge cooling in complex Langevin for QCD with heavy quarks, *Phys. Lett. B* **723**, 213 (2013).
- [29] G. Aarts and I. O. Stamatescu, Stochastic quantization at finite chemical potential, *J. High Energy Phys.* **09** (2008) 018.
- [30] G. Aarts, E. Seiler, and I. O. Stamatescu, The complex Langevin method: When can it be trusted?, *Phys. Rev. D* **81**, 054508 (2010).
- [31] G. Aarts, Lefschetz thimbles and stochastic quantization: Complex actions in the complex plane, *Phys. Rev. D* **88**, 094501 (2013).
- [32] G. Aarts, L. Bongiovanni, E. Seiler, and D. Sexty, Some remarks on Lefschetz thimbles and complex Langevin dynamics, *J. High Energy Phys.* **10** (2014) 159.
- [33] K. Fukushima and Y. Tanizaki, Hamilton dynamics for Lefschetz-thimble integration akin to the complex Langevin method, *Prog. Theor. Exp. Phys.* (2015) 111A01.
- [34] S. Tsutsui and T. M. Doi, An improvement in complex Langevin dynamics from a view point of Lefschetz thimbles, *Phys. Rev. D* **94**, 074009 (2016).
- [35] E. Witten, Analytic continuation of Chern-Simons theory, *AMS/IP Stud. Adv. Math.* **50**, 347 (2011); A new look at the path integral of quantum mechanics, [arXiv:1009.6032](https://arxiv.org/abs/1009.6032).
- [36] M. Cristoforetti, L. Scorzato, and F. Di Renzo, The sign problem and the Lefschetz thimble, *J. Phys. Conf. Ser.* **432**, 012025 (2013).
- [37] L. Scorzato, The Lefschetz thimble and the sign problem, *Proc. Sci.*, LATTICE2015 (2016) 016 [[arXiv:1512.08039](https://arxiv.org/abs/1512.08039)].
- [38] H. Fujii, D. Honda, M. Kato, Y. Kikukawa, S. Komatsu, and T. Sano, Hybrid Monte Carlo on Lefschetz thimbles—A study of the residual sign problem, *J. High Energy Phys.* **10** (2013) 147.
- [39] M. Cristoforetti, F. Di Renzo, and L. Scorzato (AuroraScience Collaboration), New approach to the sign problem in quantum field theories: High density QCD on a Lefschetz thimble, *Phys. Rev. D* **86**, 074506 (2012).
- [40] Y. Tanizaki, Lefschetz-thimble techniques for path integral of zero-dimensional $O(n)$ sigma models, *Phys. Rev. D* **91**, 036002 (2015).
- [41] H. Fujii, S. Kamata, and Y. Kikukawa, Lefschetz thimble structure in one-dimensional lattice Thirring model at finite density, *J. High Energy Phys.* **11** (2015) 078; Erratum, *J. High Energy Phys.* **02** (2016) 36; Monte Carlo study of Lefschetz thimble structure in one-dimensional Thirring model at finite density, *J. High Energy Phys.* **12** (2015) 125; Erratum, *J. High Energy Phys.* **09** (2016) 172(E).
- [42] A. Mukherjee and M. Cristoforetti, Lefschetz thimble Monte Carlo for many-body theories: A Hubbard model study, *Phys. Rev. B* **90**, 035134 (2014).
- [43] T. Kanazawa and Y. Tanizaki, Structure of Lefschetz thimbles in simple fermionic systems, *J. High Energy Phys.* **03** (2015) 044.
- [44] Y. Tanizaki, Y. Hidaka, and T. Hayata, Lefschetz-thimble analysis of the sign problem in one-site fermion model, *New J. Phys.* **18**, 033002 (2016).
- [45] T. D. Cohen, Functional Integrals for QCD at Nonzero Chemical Potential and Zero Density, *Phys. Rev. Lett.* **91**, 222001 (2003).
- [46] K. Splittorff and J. J. M. Verbaarschot, Phase of the Fermion Determinant at Nonzero Chemical Potential, *Phys. Rev. Lett.* **98**, 031601 (2007).
- [47] A. Behtash, T. Sulejmanpasic, T. Schaefer, and M. Unsal, Hidden Topological Angles and Lefschetz Thimbles, *Phys. Rev. Lett.* **115**, 041601 (2015).
- [48] P. A. Amundsen and P. H. Damgaard, Variational solutions to stochastic quantization, *Phys. Rev. D* **29**, 323 (1984).
- [49] Y. Grandati, A. Berard, and P. Grange, Variational principle in stochastic quantization and $1/N$ expansion, *Phys. Lett. B* **276**, 141 (1992); Variational $1/N$ expansion of the self-energy in stochastic quantization of the $O(N)$ Φ^4 theory, *Phys. Lett. B* **304**, 298 (1993).
- [50] J. Greensite, Comparison of complex Langevin and mean field methods applied to effective Polyakov line models, *Phys. Rev. D* **90**, 114507 (2014).
- [51] Y. Tanizaki, H. Nishimura, and K. Kashiwa, Evading the sign problem in the mean-field approximation through Lefschetz-thimble path integral, *Phys. Rev. D* **91**, 101701 (2015).
- [52] K. Fukushima and Y. Hidaka, A model study of the sign problem in the mean-field approximation, *Phys. Rev. D* **75**, 036002 (2007).
- [53] J. R. Klauder and W. P. Petersen, Spectrum of certain non-self-adjoint operators and solutions of Langevin equations with complex drift, *J. Stat. Phys.* **39**, 53 (1985).
- [54] J. Ambjorn and S. K. Yang, Numerical problems in applying the Langevin equation to complex effective actions, *Phys. Lett.* **165B**, 140 (1985).